Journal of Engineering Physics and Thermophysics, Vol. 66, No. 1, 1994

EFFECT OF THERMAL PROCESSES ON THE ACCURACY OF PRECISION FIBER-OPTIC INERTIAL SENSORS

V. É. Dzhashitov

UDC 629.12.053.531.383

A mathematical model of thermal processes and temperature errors is constructed for a promising sensor to determine the angular position and angular velocity of moving objects - a fiber-optic gyroscope (FOG). Methodological, algorithmic, and program supports are developed making it possible to carry out an automatic investigation of the functioning of an FOG exposed to temperature effects. Computational experiments and computer analysis of thermal processes and thermal drift are performed for specific design versions of the FOG, and recommendations for decrease in the temperature errors of the FOG are developed.

Introduction. Fiber-optic gyroscopes (FOG) on the basis of Sanyak interferometers with an annular coil of optical fiber find ever wider applications in navigation instruments and systems. According to [1, 2], in an FOG with phase modulation and with the use of microoptics technology the resolving power and drift amount to (0.1-0.02) deg/h which is admissible for solving problems of inertial navigation. At the same time, such a level of drift of the FOG requires one to take into account "thin" disturbing factors, among which thermal effects are a principal feature.

A complex temperature field originating in this case in the instrument exposed to these effects and varying in space and time leads to a number of changes in the optical system. Changes occur in refractive indices, scale coefficient, and in the state of polarization of the fiber. Temperature losses of the optical signal power, temperature changes in the characteristics of the photodetector, the occurrence of "drifts" due to the effects of thermophotoelasticity, etc. are possible.

The purpose of the present work is to construct an adequate mathematical model of the thermal processes and temperature errors of an FOG, to develop the methodological, mathematical, algorithmic and program supports that make it possible to conduct an automatic analysis of the functioning of the FOG under the conditions of temperature effects, and to work out recommendations for decreasing its temperature drift and thus to increase the accuracy of the sensor.

The statement of the problem involves the following basic stages:

I) construction of a mathematical model of thermal processes in an FOG to calculate and analyze three-dimensional nonuniform temperature fields in it;

II) construction and analysis of the mathematical model of the drift of an FOG due to the nonuniformity and nonstationary character of the temperature field of the sensor;

III) development of the algorithmic and program supports of the computer analysis of thermal processes and temperature errors of an FOG in a single complex;

IV) execution of computational experiments, analysis of thermal processes and temperature "drifts" of specific design versions of the sensor, and recommendations for their reduction.

Let us consider the basic results obtained.

Stage I. To calculate the temperature field of an FOG, a modified method of "elementary balances" is used. The instrument is "divided" into a number of finite "elementary" geometric forms whose centers are the points of computation.

Branch of the A. A. Blagonravov Institute of Mechanical Engineering, Saratov. Translated from Inzhenerno-Fizicheskii Zhurnal, Vol. 66, No. 1, pp. 61-68, January, 1994. Original article submitted May 13, 1992.

1062-0125/94/6601-0055$12.50

The basic algorithm derived for each of the computational point on the basis of the fundamental conservation and heat conduction laws has the form

$$T_{\tau+\Delta\tau} = \left[1 - \frac{\Delta\tau}{c} \left(\sum_{j=1}^{n} q_j + \sum_{j=n+1}^{m} q_{jc} \right) \right] T_\tau + \frac{\Delta\tau}{c} \left(\sum_{j=1}^{n} T_j q_j + T_{\text{en}} \sum_{j=n+1}^{m} q_{jc} + Q \right). \tag{1}$$

The basic algorithm (1) realized on a computer makes it possible to calculate the temperature field at each computational point in the course of time. The number of computational points may range from several tens to several thousands. The calculation of the temperature field was tested on a number of sophisticated instruments and systems of precision instrument engineering [4-6] and proved to be a rather simple, all-purpose, reliable, and accurate method. Thus, the standard error of the predicted and experimental data for a number of computational points on the order of several hundreds does not exceed 10% under unsteady conditions and is less than 10% in steady temperature regimes.

Stage II. As the information analysis showed, one of the basic reasons for the thermal drift of the FOG is [1, 2, 7] the thermally induced nonreciprocity in the fiber circuit of the instrument. Such nonreciprocity sets in if the corresponding wave fronts of two opposite beams traverse the same region in the fiber for different periods of time. Equating the phase shift induced by temperature gradients to the Sanyak phase shift, we can determine, according to [7], the "apparent" angular velocity of rotation of the FOG (the angular velocity of the temperature drift) in the form

$$\Omega_T = \frac{1}{4m^* \sum_{i=1}^{n^*} S_{bi}} \int_0^L \left(\frac{\partial n_1}{dT} + n_1 \alpha \right) n_1 (2s - L) \frac{\partial T}{\partial \tau} ds. \tag{2}$$

Let us consider the possible cases of (2). We shall assume [8, 9] that

$$n_1 = n_{10} + hT(s, \tau), \tag{3}$$

$$T(s, \tau) = T^0 f(s, \tau), \tag{4}$$

If the function $f(s, \tau)$ characterizing the temperature field configuration admits a separation of variables

$$f(s, \tau) = f_1(\tau) f_2(s) \tag{5}$$

and $f_2(s)$ can be presented in the form of the Fourier series

$$f_2(s) = \frac{a_0}{2} + \sum_{i=1}^{\infty} \left(a_i \cos \frac{i\pi s}{l} + b_i \sin \frac{i\pi s}{l} \right), \tag{6}$$

then Eq. (2) will yield

$$\Omega_T(\tau) = - T^0 f_1(\tau) [h + \alpha n_{10}] n_{10} m^* n^* \sum_{i=1}^{\infty} b_i / i. \tag{7}$$

If $f(s, \tau)$ (the function determined in the region $0 \le \tau \le 2\tau^*$, $0 \le s \le 2l$) does not admit a separation of variables and its partial time derivative is representable in the form of the double Fourier series

$$\frac{\partial f}{\partial \tau} = \tilde{f}(s, \tau) = \frac{f_0(s, \tau)}{2\tau^*} = \frac{1}{2\tau^*} \left\{ \frac{\tilde{a}_{00}}{4} + \left[\sum_{i=1}^{\infty} \left(\tilde{a}_{0i} \cos \frac{i\pi s}{l} + \right. \right. \right.$$

$$+ \tilde{b}_{0i} \sin \frac{i\pi s}{l}\Bigg)\Bigg]\Bigg/2 + \Bigg[\sum_{j=1}^{\infty}\Bigg(\tilde{a}_{j0} \cos \frac{j\pi\tau}{\tau^*} + \tilde{c}_{j0} \sin \frac{j\pi\tau}{\tau^*}\Bigg)\Bigg]\Bigg/2 +$$

$$+ \sum_{j=1}^{\infty}\sum_{i=1}^{\infty}\Bigg[\tilde{a}_{ji} \cos \frac{j\pi\tau}{\tau^*} \cos \frac{i\pi s}{l} + \tilde{b}_{ji} \cos \frac{j\pi s}{\tau^*} \sin \frac{i\pi s}{l} +$$

$$+ \tilde{c}_{ji} \sin \frac{j\pi\tau}{\tau^*} \cos \frac{i\pi s}{l} + \tilde{d}_{ji} \sin \frac{j\pi\tau}{\tau^*} \sin \frac{i\pi s}{l}\Bigg]\Bigg\}, \qquad (8)$$

then Eq. (2) will give

$$\Omega_T(\tau) = - T^0 (h + \alpha n_{10}) n_{10} m^* n^* \times$$

$$\times \Bigg\{\sum_{i=1}^{\infty}\Bigg[\tilde{b}_{0i} + 2\sum_{j=1}^{\infty}\Bigg(\tilde{b}_{ji} \cos \frac{j\pi\tau}{\tau^*} + \tilde{d}_{ji} \sin \frac{j\pi\tau}{\tau^*}\Bigg)\Bigg]\Bigg/i\Bigg\}\Bigg/4\tau^*. \qquad (9)$$

Analyzing analytical relations (7) and (9), which is the basis of the mathematical model of the temperature drift of the FOG, we note that:

1) relations (7) and (9) extend the familiar formulas to the case of an arbitrary configuration of the temperature field. Thus, when the temperature along the fiber varies linearly the expressions suggested in [2, 7] for the temperature drift of the FOG follow from Eqs. (7) and (9) as a particular case. The representation of the temperature field in the form of Fourier series permits one, by using the methods of harmonic analysis, to apply these relations to any temperature field configurations determined analytically, numerically, or experimentally;

2) the temperature drift of the FOG occurs at a nonstationary temperature ($\partial f/\partial\tau \neq 0$);

3) according to [9], the temperature coefficient h of the refractive index can be either positive or negative depending on the type of fiber. According to Eqs. (7) and (9), this affords additional possibilities for minimizing the temperature drift of the FOG;

4) Eqs. (7) and (9) involve only the coefficients of the Fourier series which are "responsible" for the temperature being an odd function of s, i.e., if the temperature is an even function of s (symmetric about the axis which is normal to the longitudinal axis of the fiber and which passes through its center), then the drift is at a minimum;

5) the specificity of the real designs of an FOG [1, 2] is the fact that fiber is wound on a bobbin in the form of a cylindrical coil. In this case, the effect of temperature drops along the cylindrical coordinates R, φ, and z is manifested in periodic nonuniform heating of the fiber over different portions. In other words, "thermal bands" of different structure are observed along the fiber length that affect differently the drift of the FOG. For simplicity we will assume that constant temperature drops are observed in the instrument up to the middle of the fiber coil along the respective coordinates.

Figure 1 presents the temperature drops of the cylindrical fiber coil unrolled as a single thread, as well as the calculated values of $\Sigma\, b_i/i$ to which the drift of the FOG is proportional. As is seen from the figure, the temperature drops ΔT_R along the radius of the cylindrical coil are most unfavorable as concerns the effect on the temperature drift (the graph most asymmetric about the axis normal to the longitudinal axis of the fiber and passing through its center);

6) as follows from Eqs. (7) and (9), a smaller drift is caused by "thermal bands" of high frequency, because smaller coefficients $\Sigma\, b_i/i$ precede the higher harmonic in the Fourier series.

Stage III. To make use of computer assistance in investigations of the temperature drift of real designs of an FOG following the scheme "drawing-temperature field-temperature drift," it is necessary to work out the corresponding algorithmic and program supports.

Here, two approaches are possible.

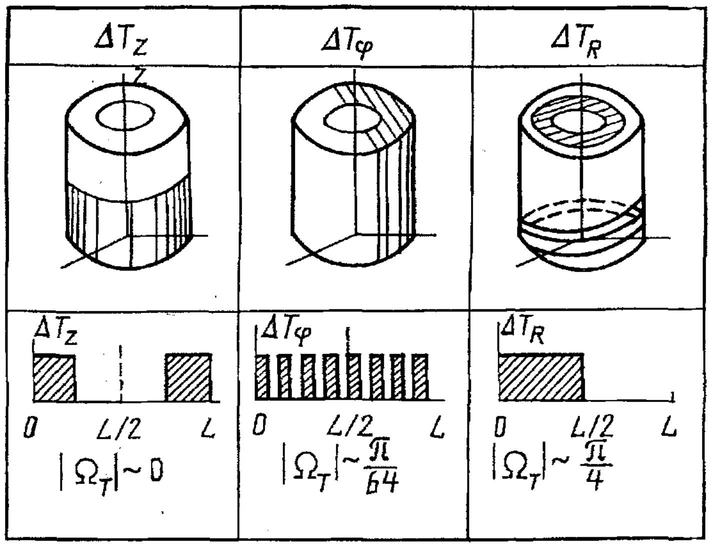

Fig. 1. Effect of temperature drops over the fiber coil on the drift of the FOG.

The first (autonomous) approach is to calculate the temperature field of the instrument separately with the aid of algorithm (1) at a given number of computational points (including the fiber coil). The resulting function of temperatures in the cylindrical coordinates $T = T(R, \varphi, z, \tau)$ is recalculated by the familiar formulas for a helical line into the temperature function depending on the angular position $T = T(s, \tau)$. Using the harmonic analysis methods, the temperature function obtained is represented in the form of Fourier series of type (6) or (8). The drift of the FOG due to the thermally induced nonreciprocity is calculated from Eq. (7) or (9).

One of the drawbacks of this approach is that for long fibers (the length of the real fibers in the FOG is on the order of 1000 m) collected into a compact coil the "thermal bands" may have a high frequency, and one has to drive the range of Fourier series expansion of the temperature function into a very large number of portions (of the order of 2500 for the real radii of the FOG coils) which will entail computational difficulties in the harmonic analysis. Moreover, such an approach does not permit one to carry out the schematic-algorithmic compensation of the temperature drift in the instrument.

The second approach (calculation of the temperature drift together with the temperature field of the FOG) is free from the above disadvantages and amounts to the following.

The temperature field of the FOG is calculated at the computational points at each time instant with the step $\Delta\tau$ using algorithm (1). Then values of the temperatures T_j, $T_j^{\tau+\Delta\tau}$ are selected that correspond to the computational points of the fiber coil.

The values of $\dot{T}_j = (T_j^{\tau+\Delta\tau} - T_j)/\Delta\tau$, $\dot{T}_{\min} = \min(\dot{T}_j)$, and $\Delta\dot{T}_j = \dot{T}_j - \dot{T}_{\min}$ are calculated. Then, using the formulas for the helical line, we replace the variable s by φ. The integration interval $[0, L]$ is divided into portions corresponding to the computational points at which the temperature field is determined.

On the basis of Eq. (2), over each of the portions the component Ω_{Ti} of the temperature drift of the FOG and the total drift $\Omega_T = \Sigma\, \Omega_{Ti}$ are determined with account for the substitution of variables. The above algorithm, used at discrete time instants with the computation step $\Delta\tau$, gives the temperature field of the FOG $T = T(R, \varphi, z, \tau)$ and simultaneously the values of the temperature drift $\Omega_T = \Omega_T(\tau)$.

The formulas, relationships, and algorithms considered were implemented in a complex of programs written in the algorithmic FORTRAN language and adapted to an IBM PC/AT.

The complex developed incorporates the following basic program modules:

a) the basic program VOGTE to calculate three-dimensional nonstationary nonuniform temperature fields of the instrument with heat emitting elements taking into account the deterministic and random temperature effects;

b) the subprogram-function GJ to calculate the temperature drift of the instrument;

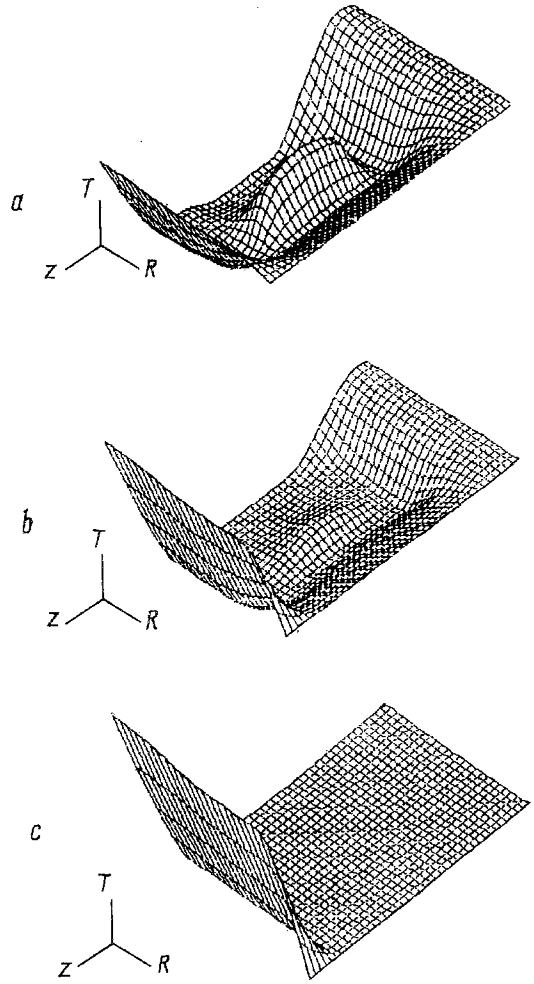

Fig. 2. Topograms of the temperature fields (°C) of the FOG in the section φ = const: a) at the 3rd minute of thermal regime (T_{max} = 40.92°C; T_{min} = 24.35°C); b) at the 9th minute (T_{max} = 42.58°C; T_{min} = 20.90°C); c) at the 30th minute (T_{max} = 45.44°C; T_{min} = 20.01°C).

c) the subprograms for visualizing the results of simulation that use a package of graphical programs GRAFOR [10] for graphical representation of three-dimensional temperature fields (in the form of topograms) and of the current parameters of thermal processes and the temperature drift of the instrument.

Stage IV. The mathematical model constructed and the algorithmic and program supports developed made it possible, with the aid of computational experiments, to investigate thermal processes and errors of specific design versions of FOG. The temperature field of a FOG was calculated at 371 computational points throughout the instrument volume. The simulation of one minute of the thermal operational regime of the instrument corresponds to two minutes of computer time for IBM PC/AT-386.

In Fig. 2 the topograms are presented for the temperature fields of the FOG (with the fiber coil insulated from the blocks of electronics and without a system of thermal control) in the section φ = const at different time instants in the case of a stepwise change in the environmental temperature from 40 to 20°C. As is seen from Fig. 2, the cooling of the sensor is a nonuniform process and the temperature field in the FOG has an essentially nonuniform character in transient regimes (the 3rd and 9th minutes) due to the constructional nonuniformity of the sensor and various thermophysical characteristics of the materials of which its elements are made. In the steady regime (30th minute) substantial superheating is observed for the zones in which the main heat emitting sources are located (blocks of electronics) as compared with other zones (e.g., of the fiber coil).

In Fig. 3 the transient thermal processes and temperature drift curves of the instrument are presented for deterministic and random changes in the environmental temperature.

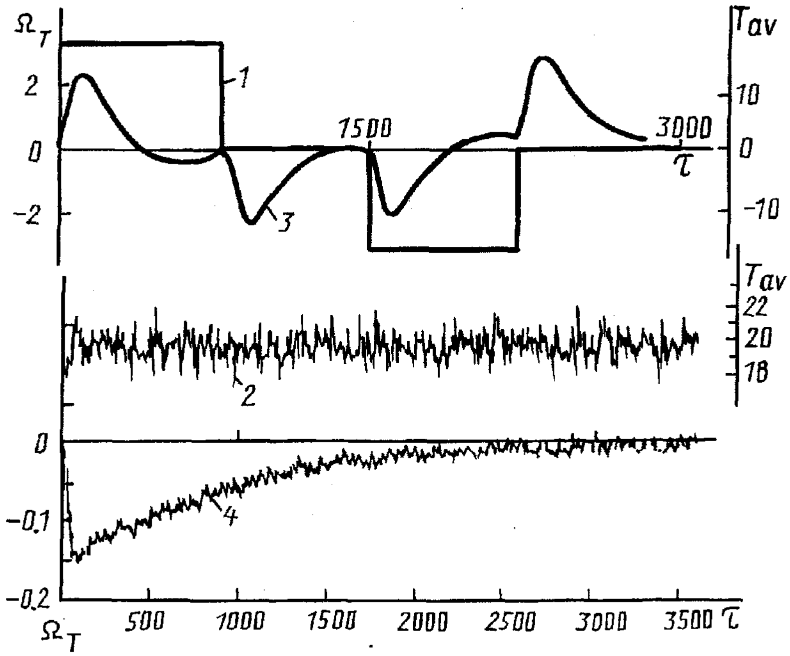

Fig. 3. Current values of temperatures and angular velocity of the temperature drift of the FOG: 1, 2) environmental temperature, °C; 3, 4) angular velocity of temperature drift Ω_T, deg/h. τ, sec.

As the mathematical simulation and the analysis of the results obtained show, the character of the calculated curves of the instrument drift corresponds qualitatively to that of the experimental drift curves of a typical FOG presented in [1] which also confirms the adequacy of the model constructed. As is seen from Fig. 3, the stepwise changes in the environmental temperature by 20°C induce a dynamic drift of the FOG at a level of 3 deg/h which is essential for inertial sensors. The influence of the internal heat sources of power 2 W is responsible for the deterministic angular velocity of the gyroscope "drift" with the maximum value at the level of 0.16 deg/h.

Random continuous change in the environmental temperature in the range with the standard deviation $\sigma_m = 1$°C causes a random drift with the standard deviation 0.01 deg/h. According to the data of mathematical simulation, the time of thermal readiness of an FOG without the system of thermal control is not less than 30 min, which is also a very appreciable value for this class of sensors.

The investigations carried out with the aid of the constructed mathematical model show that some basic ways are possible for minimizing the temperature drift of an FOG and improving its accuracy and other characteristics:

(1) insulation of the fiber coil from the surrounding medium and internal heat releasing sources. Here, one will probably have to solve an optimization problem, since the complete insulation greatly complicates the structure and can lead to internal overheating of the fiber coil of the FOG (laser radiation sources produce milliwatt heat fluxes, but in a completely insulated fiber coil the power may be substantial);

(2) development of a system of thermal control of the FOG ensuring a reduction in the time for thermal readiness, and maintaining a given absolute temperature, minimal radial temperature drops, and their time derivatives in a fiber coil;

(3) schematic-algorithmic compensation of temperature drift. Basic algorithms for constructing a mathematical model are put into the airborne computer. The values of temperature are recorded from thermal sensors located in the FOG in a certain way and are processed according to the algorithms used; the signal is calculated, which is proportional to the angular drift velocity and is fed with the opposite sign to the optical system compensating for the gyroscope "drift."

The constructed mathematical model of the temperature drift of a fiber-optic gyroscope and the algorithmic and program supports developed permit one to simulate the possible ways for reducing this drift.

Conclusions. In the present work a mathematical model of the temperature drift is constructed for a promising precision transducer of primary information on the angular velocity and angular position of moving objects — a fiber-optic gyroscope.

The practical significance of the work consists in the fact that the realization of the constructed mathematic model in the form of algorithms and programs permits one at the stage of design to conduct computer-aided investigations of complex design version of an FOG from drawing to the calculation of the temperature field and then to the calculation and analysis of the temperature errors of the instrument.

The analysis of the optical and thermal physical processes in the FOG and the analytical relationships obtained for the temperature errors of the FOG as functions of its design parameters and temperature field configuration represented by the Fourier series in conjunction with the computational experiments performed on the model constructed make it possible to determine ways for increasing the accuracy of the instrument.

NOTATION

T_τ, $T_{\tau+\Delta\tau}$, values of temperatures at a given computational point at present and successive time instants, respectively; T_j, values of temperatures at computational points adjacent to that given; T_{en}, environmental temperature; c, heat capacities of "elementary" volumes corresponding to computational points of the model; q_j, q_{jc}, thermal conductivity coefficients; Q, heat release power of heat sources; $\Delta\tau$, time step in temperature computation; n, number of "internal" thermal couplings of elementary volumes adjacent to that given; m, total number of thermal couplings of given elementary volume; n^*, number of turns in the wound layer of fiber coil along radius r; m^*, number of turns in the winding layer along the height z; S_{bi}, area of ith turn; n_1, refractive index of fiber core; α, coefficient of linear thermal expansion of fiber; s, angular position of fiber; τ, time; $T(s, \tau)$, temperature function; $L = 2l$, length of fiber loop; ΔT_z,ΔT_φ,ΔT_R, temperature drops in fiber cylindrical coil along respective coordinates; n_{10}, rated value of fiber core refractive index; h, temperature coefficient of refractive index.

REFERENCES

1. T. Okosi, K. Okomoto, and M. Otsu, Fiber-optic Sensors (edited by T. Okosi) [Russian translation], Leningrad (1990).
2. A. G. Sheremetiev, A Fiber Optic Gyroscope [in Russian], Moscow (1987).
3. G. N. Dul'nev, V. G. Parfenov, and A. V. Sigalov, Methods for Calculating the Thermal Regime of Instruments [in Russian], Moscow (1990).
4. V. É. Dzhashitov and V. M. Pankratov, Izv. VUZov, Priborostroenie, No. 4, 80-83 (1983).
5. V. É. Dzhashitov, V. M. Pankratov, and A. B. Suchkov, Probl. Mashinostr. Nadyozhn. Mashin, No. 4, 106-111 (1990).
6. V. É. Dzhashitov and A. B. Suchkov, Inzh.-Fiz. Zh., **61**, No. 4, 692 (1991).
7. D. M. Hupe, Appl. Opt., **19**, No. 5, 654-655 (1980).
8. M. G. Voitik, B. G. Gorshkov, et al., Zh. Tekh. Fiz., **53**, No. 9, 1791-1796 (1983).
9. G. B. Hocker, Appl. Opt., **18**, No. 9/I May, 1445-1448 (1979).
10. Yu. M. Boyakovskii, V. A. Galaktionov, and T. N. Mikhaikova, GRAFOR. Graphic Extension of Fortran [in Russian], Moscow (1985).